This article is published as part of the *Dalton Transactions* themed issue entitled:

Coordination chemistry in the solid state

Guest Editor Russell E. Morris

Published in Issue 14, Volume 41 of *Dalton Transactions*

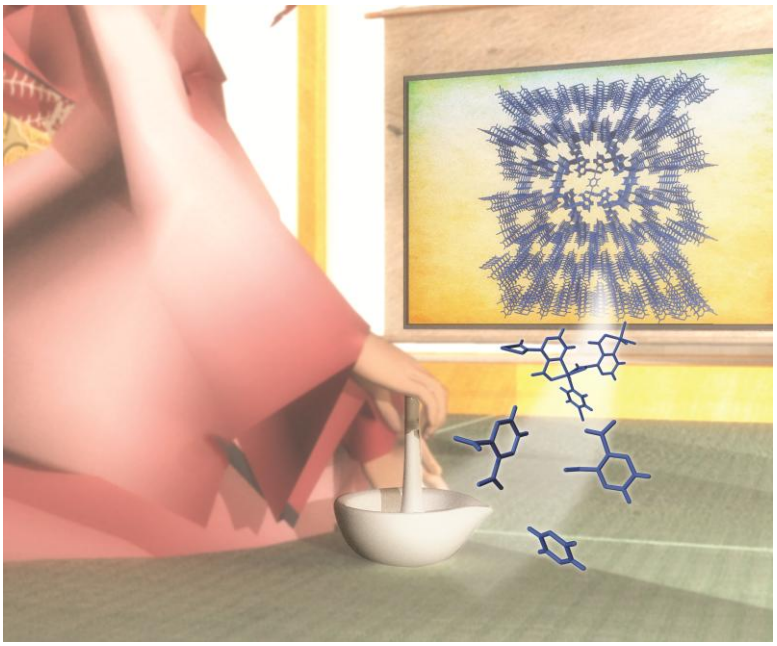

Articles in this issue include:

Visit the *Dalton Transactions* website for the latest cutting inorganic chemistry
www.rsc.org/publishing/journals/dt/

Dalton Transactions

Dynamic Article Links

Cite this: *Dalton Trans.*, 2012, **41**, 4255

www.rsc.org/dalton

PAPER

In situ selective *N*-alkylation of pendant pyridyl functionality in mixed-valence copper complexes with methanol and copper(II) bromide†

Da-Qian Feng, Xiao-Ping Zhou, Ji Zheng, Guang-hui Chen, Xiao-Chun Huang and Dan Li*

Received 2nd November 2011, Accepted 6th February 2012
DOI: 10.1039/c2dt12081j

The reactions of $CuBr_2$ with pyridyl 2,2′:6′,2″-terpyridine ligands in methanol yielded four copper complexes under solvothermal conditions. The self-assembly processes were accompanied by designing bitopic precursor ligands and increasing the stoichiometric metal–ligand ratio. In the four resulting complexes, the pendant pyridyl groups of pyridylterpyridine were selectively *in situ N*-methylated and yielded the 4′-(*N*-methylpyridinium)-2,2′:6′,2″-terpyridine cations, including the 2-position pyridyl group which is difficult to be *N*-alkylated due to the steric problem. Partial divalent copper atoms were reduced to cuprous ones in the solvothermal reactions, which made the mixed-valence copper atoms coexist in each compound. The mixed-valence complexes have a varied dimensionality (from 2D to 0D) and the Cu^IBr cluster, which can be controlled by changing the metal–ligand ratio. Theoretical studies show that the nucleophilic attack of the nitrogen atom in the pendant pyridyl is more facile than others of terpyridine. A possible mechanism was also proposed.

Introduction

In situ metal–ligand reactions under solvo(hydro)thermal conditions are of topical interest in coordination chemistry and organic chemistry. As a powerful non-conventional approach, lots of unusual metal–ligand reactions have been found in high pressure and at relatively high temperature.[1–8] Some reaction products in such conditions may be inaccessible by traditional organic synthesis.[1,2] *N*-alkylation of amine is one of the most fundamental and important reactions in synthetic organic chemistry. The normal method for *N*-alkylation is to use alkyl halides, which is undesirable from an environmental point of view. Introducing alcohols as substitutes should be more attractive. However, the actualization of the *N*-alkylation processes usually needs expensive Ru or Ir organometallic catalysts.[9,10] We and others have developed new *in situ N*-alkylation reactions including *N*-alkylation of triazole,[11] pyridine-4-thiol,[12] 4,4′-bipyridine[13] and 4-(4-aminobenzyl)benzenamine[14] using alcohols in the presence of cheap metal halides under solvothermal conditions.

As one of the most important tridentate ligands, terpyridine and its subsequently substituted analogues have been widely investigated in coordination chemistry. Constable *et al.* implemented a systematic investigation of *N*-alkylation of a series of mononuclear complexes of 4′-(2-pyridyl)-, 4′-(3-pyridyl)- and 4′-(4-pyridyl)-2,2′:6′,2″-terpyridine using CH_3I as alkylating agents.[15,16] They found that the pendant pyridyl groups in the former two terpyridine complexes underwent partial *N*-alkylation and obtained mono- and bis-*N*-methylated derivatives even in harsher reaction conditions (higher temperature, longer time and excess of CH_3I) due to sterical hindrances. We are interested in constructing coordination polymers using 2,2′:6′,2″-terpyridine and its derivatives as linkers, particularly functionalizing the 4′-position of the central pyridine of terpyridine to bring a pendant pyridyl donor site.[17–21] The pendant 4-pyridyl functionality terpyridines are employed as rational starting materials for *in situ* alkylation reactions. On the other hand, it has been reported that Cu^{II} ions can be reduced to Cu^I by 4,4′-bipyridine and pyridine derivatives under hydrothermal conditions.[17] It is possible to design bifunctional precursory ligands which are capable of accommodating the coordination modes of metal ions and active organic reaction. Our strategy is to construct building blocks through selective *N*-alkylation reactions of pendant pyridyl functionality *in situ*. We synthesized a series of mixed-valence copper complexes $[(Cu^{II}Br_2\mathbf{L1}Me)^+(Cu^I_4Br_5)^-]_n$ (**1**), $[(Cu^{II}Br_2\mathbf{L1}Me)^+(Cu^I_3Br_4)^-]_n$ (**2**), $[(Cu^{II}Br_2\mathbf{L1}Me^+)_2(Cu^IBr_2^-)_2]$ (**3**), and $[(Cu^{II}Br_2\mathbf{L2}Me)^+(Cu^I_{2.68}Br_{3.68})^-]_2$ (**4**) (**L1** = 4′-(4-pyridyl)-2,2′:6′,2″-terpyridine, **L2** = 4′-(2-pyridyl)-2,2′:6′,2″-terpyridine, Chart 1). The Cu^I–Cu^{II}

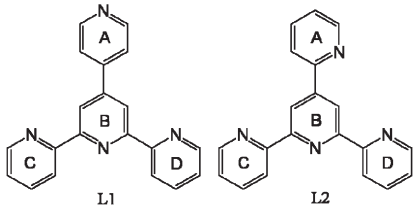

Chart 1

Department of Chemistry, Shantou University, Guangdong 515063, P. R. China. E-mail: dli@stu.edu.cn

† Electronic supplementary information (ESI) available. CCDC reference numbers 806444–806447. For ESI and crystallographic data in CIF or other electronic format see DOI: 10.1039/c2dt12081j

compounds were obtained by reactions of corresponding terpyridines with $CuBr_2$ in methanol. In these compounds, all the pendant pyridyl groups are *in situ* *N*-methylated selectively, while the other three pyridyl groups chelate Cu^{2+} centers. The advantage of using alcohols instead of alkyl halides is obvious because alcohols are not only cheaper and more ready available, but are also environmental friendly.

Results and discussion

In situ *N*-methylation products

Complexes **1–4** were obtained by reacting $CuBr_2$ with **L1** or **L2** under identical solvothermal conditions (methanol as solvent, temperature at 140 °C, see Experimental section). X-ray single-crystal analyses reveal that complexes **1–4** contain varied $Cu^{I}Br$ anionic aggregations (see below for structure description) and 4′-(*N*-methylpyridinium)-2,2′:6′,2″-terpyridine ligands, where the pendant pyridyl groups were selectively *N*-methylated, chelating to Cu^{II} atoms. The distances between the carbon atoms of methyl groups and the nitrogen atoms of the pyridinium are 1.454(13)–1.494(13) Å, which are typical C–N bonds for *N*-alkylated pyridinium.[15,16]

The *in situ* *N*-methylation of the pendant pyridyl group was also proved by the featuring C–H stretching vibrations of the methyl groups (2927 cm^{-1}–2850 cm^{-1}) in their IR spectra. The UV-vis absorption data (Fig. S1, ESI†) of reaction filtrates in CH_3OH solutions show that the reaction products are significantly different from the starting materials. The spectrometry further demonstrates that the *N*-alkylation approach with alcohol under solvothermal conditions is successful and practicable. In **1–4**, the planar character of the tridentate motif of the terpyridyl ligands is critical in keeping the divalent copper ion at this site, *in situ* methylation of the monodentate pyridyl to methylpyridinium was observed. Thermogravimetric analyses of all compounds in argon demonstrate the mass loss as shown in Fig. S2 (ESI†) indicating the complexes are thermally stable up to 300–400 °C.

Crystal structures

Complex **1** features two dimensional grid-like networks based on the linkage of $Cu^{II}Br_2$**L1**Me^+ sections to $[Cu_4Br_5^-]_n$ inorganic anionic chains. The asymmetric portions of the unit cell contains 2.5 copper atoms (Cu1, Cu2 and Cu3, Cu1 located on the C_2 axis with sites occupancy 0.5), half of the **L1**Me^+ cation, and 3.5 Br^- anions (Br1, Br2, Br3, and Br4, Br4 is disordered with sites occupancy 0.5). The divalent Cu1 is chelated by the three nitrogen atoms and bound by additional two Br^- ions, adopting a distorted trigonal bipyramid geometry (Cu–N 1.930(2)–2.0235 (3) Å, Cu–Br 2.517(3) Å; N–Cu–N 79.849(3)°, N–Cu–Br 94.781(4)–126.52(3)°, Br–Cu–Br(1) 106.95(5)°). The two Cu2 and two Cu3 atoms are bound by four Br^- ions to construct a distorted cubic Cu_4Br_4 cluster (Fig. 1a), in which the Br ions adopt a μ_3-bridging mode and copper atoms adopt a tetrahedron geometry (completed by an additional μ_2-Br atom, Br1 or Br4, (Cu–Br 2.473(2)–2.669(2) Å), respectively. The tetrahedron geometry of Cu2 and Cu3 indicates that they are cuprous atoms, in accordance with the requirement of charge balance. The redox

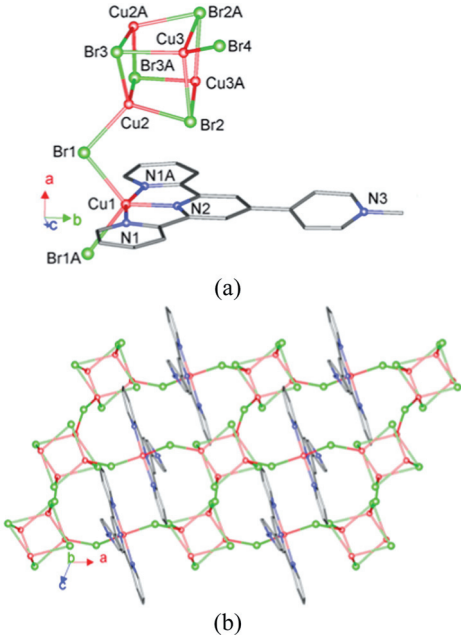

Fig. 1 The structure of **1**. (a) View of the $Cu^{II}Br_2$**L1**Me^+ sections and Cu_4Br_4 cluster. (b) 2D grid-like network view along the *b* axis. Hydrogen atoms are omitted for clarity.

reaction for copper ions often occurs under hydro(solvo)thermal conditions.[1] The Cu_4Br_4 clusters are linked by the μ_2-Br4 atoms to form a 1D anionic $[Cu_4Br_5^-]_n$ chain. Then the chains are further extended to a 2D grid-like network by the $Cu^{II}Br_2$**L1**Me^+ through Cu–Br coordination bonds, as shown in Fig. 1b. Although distorted cubic Cu_4Br_4 clusters were well documented, being embedded into a mixed-valence 2D network is rarely reported.

Similar to **1**, complex **2** also contains the $Cu^{II}Br_2$**L1**Me^+ fragment and anionic $Cu^{I}Br$ chains. However, both of them have their differences. The pendant pyridinium ring twist at an angle of 34.2° to the central pyridyl ring in **2**, and the angle in **1** is 14.1°. Unlike that adopting a trigonal bipyramid geometry in **1**, the divalent Cu1 atom in **2** adopts a more likely distorted square pyramidal geometry (Fig. 2a). The three N atoms and one Br atom (Br1) bonding to the Cu1 atom form the square base (Cu–N, 1.9366(1)–2.0246(1) Å, and Cu–Br, 2.3352(1) Å), and an additional Br2 atom occupies the apex through a lengthened coordination bond (Cu1–Br2 2.8765(2) Å) to complete the square pyramidal geometry. The cuprous atoms binding with Br atoms form a Cu_3Br_3 cluster (Fig. 2a). Similar Cu_3Br_3 clusters were found in the previous reported compounds Cu_3(2,3-dmpz)$_2Br_3$[22] and Cu_3Br_3(dpmt)$_2$.[23] The trinuclear clusters were further linked by the bridging Br atoms (Br6) to form a $[Cu_3Br_4]^-_n$ anionic chain like in **1** and then extend to a triple-rung ladder structure. Interestingly, only one Br atom (Br2) for each $Cu^{II}Br_2$**L1**Me^+ bridges to the $[Cu_3Br_4^-]_n$ chain (Br1 as a terminal coordination) leading to the formation of a ribbon structure rather than a 2D one.

Complex **3** features a relatively simple oligonuclear structure compared with the polymeric structures in **1** and **2**, as shown in Fig. 3. The **L1**Me^+ chelates the divalent Cu1 with three nitrogen atoms like those in **1** and **2**, and the divalent Cu1 adopts a

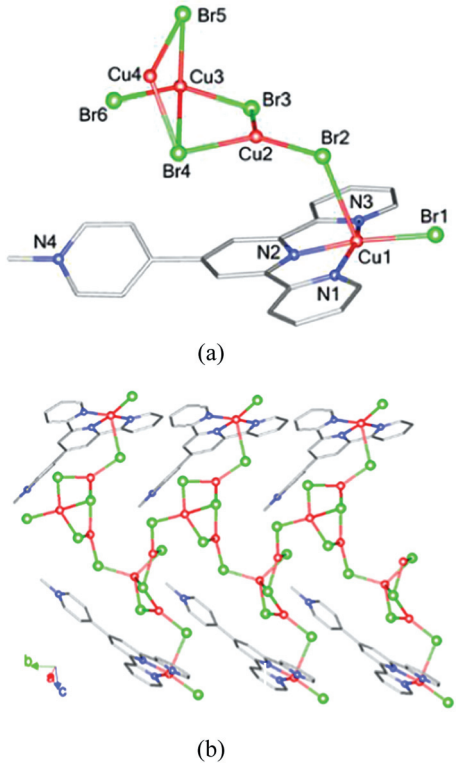

Fig. 2 The structure of **2**. (a) The asymmetric unit of complex **2**. (b) The 1D ribbon structure of **2**. Hydrogen atoms are omitted for clarity.

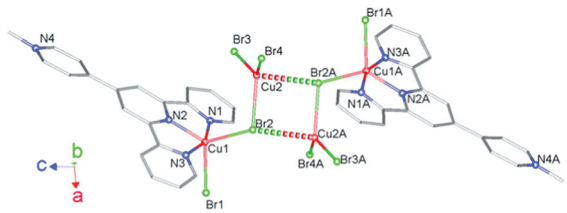

Fig. 3 The structure of **3**. Hydrogen atoms are omitted for clarity.

distorted trigonal bipyramid geometry completed by two additional Br atoms (Cu–N, 1.9646(2)–2.0326(3) Å, Cu–Br, 2.4757(3)–2.4897(3) Å, N–Cu–N 79.13(1)–79.43(1)°, N–Cu–Br 91.46(1)–120.04° and Br1–Cu1–Br2 109.38(1)°). The positive $Cu^{II}Br_2$**L1**Me^+ is linked to the $Cu^{I}Br_2^-$ anionic unit (Cu–Br, 2.3722(3)–2.2799(3) Å) through Br2 bridging to Cu2 (2.5243(3) Å), and then a dinuclear complex is formed. Interestingly, the dinuclear complex is further interacted to an adjacent dinuclear complex forming a tetranuclear adduct with two weaker Cu–Br coordination bonds (3.0047 (4) Å, Fig. 3). The bond distance is just slightly shorter than the sum of the Van der Waals radius of Cu (1.40 Å) and Br (1.85 Å).

In the syntheses of complexes **1–3**, we try to tune the structures (*e.g.*, dimensionality and the size of $Cu^{I}Br$ cluster) by changing the metal–ligand ratio. In complexes **1–3**, the dimensionality decreases from 2D to 0D and the $Cu^{I}Br$ cluster size decreases from tetranuclear to mononuclear when the metal–ligand ratio increases. On the other hand, the metal–ligand ratios in the products are in large disagreement with the ratios in the starting reagents. The ratios of $CuBr_2$–**L1**Me^+ in products **1–3** are degressive from 5 : 1 to 2 : 1 while the reacting ratios of

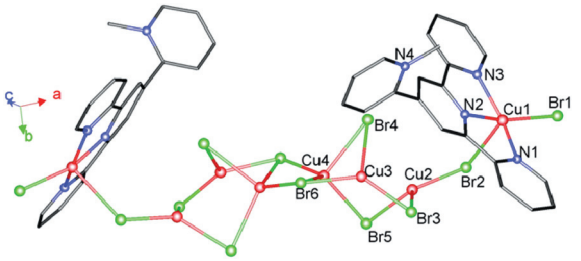

Fig. 4 The structure of **4**. Hydrogen atoms are omitted for clarity.

$CuBr_2$–**L1** increase from 2 : 1 to 8 : 1. No doubt the metal–ligand ratio (stoichiometry) plays an important role in controlling the assembly of the complexes. However, in the reported results, the metal–ligand ratios in the products are always consistent with the reacting ratios.[24–26] Here, this difference may be caused by the large excess of Cu^{2+} atoms, which affect the Cu^+ and Br^- aggregations. Under the same solvothermal conditions, the quantity of Cu^+ through reducing Cu^{2+} will probably be identical. Therefore, the non-reducing Cu^{2+} atoms (partial Cu^{2+} atoms are coordinated by the **L1**Me^+) in the reacting system during the formation of **3** will largely exceed those used than when forming **1** (probably 4 fold or more). The excess non-reacting Cu^{2+} may disturb the formation of the $Cu^{I}Br$ anionic cluster and the self-assembly of the resulting complexes will take place through electrostatic interaction. For example, the large CuBr anionic clusters may hardly form when it is surrounded by abundant Cu^{2+} ions (the Cu^{2+} ions are probably preferred more than Cu^+ because of the more positive charge). Such a condition leads to the lower dimensionality, smaller CuBr anionic cluster and a lower metal–ligand ratio like in **3**.

The synthesis of complex **4** is similar to **2** except replacing **L1** with **L2**. In the structure of **4**, two $Cu^{II}Br_2$**L2**Me^+ units are bridged by an oligonuclear cuprous bromide cluster, as shown in Fig. 4. The pendant pyridyl of **L2** was also *N*-methylated like **L1** in complexes **1–3**. The divalent Cu1 displays a distorted square pyramidal coordination geometry (similar to the structure of complex **2**), which is comprised of three N donors from the terpyridine ligand and two bromine ions (Cu–N, 1.950(6)–2.050 (7) Å, Cu–Br, 2.3734(14)–2.7520(14) Å). The dihedral angle between the pendant pyridinium and the central pyridyl of **L2**Me^+ is 78.45°, which approaches a vertical angle. The value is obviously larger than the corresponding dihedral angle value of **L1**Me^+ in complexes **1–3** (10.51° to 34.2°) and the non-*N*-alkylated **L2** in a previous reported mixed-valence complex $[Cu_2(\mathbf{L2})(SCN)_3]_n$ (12.7°).[17] The large twisting of the pendant pyridinium ring avoids the steric problem, and helps implement the *N*-methylation on the 2-position of the pyridyl group. This structural feature indicates that the **L2** needs additional energy to rotate the pendant ring to finish the *N*-methylation, and also visually shows the difficulty of *N*-methylation of **L2**. This is consistent with the difficult *N*-methylation of $[Ru(\mathbf{L2})_2][PF_6]_2$ in the presence of >1000-fold excess of CH_3I.[15] The central copper bromide cluster between the two $Cu^{II}Br_2$**L2**Me^+ sections was slightly intricate. Both Cu2 and Cu4 atoms disorder with two positions (with a ratio of 0.677 : 0.323, and 0.51 : 0.49, respectively), when Cu3 and Br3 atoms are only partially occupied (refined as a 0.677 site occupation). Therefore, the overall formula of complex **4** determined from X-ray diffraction can

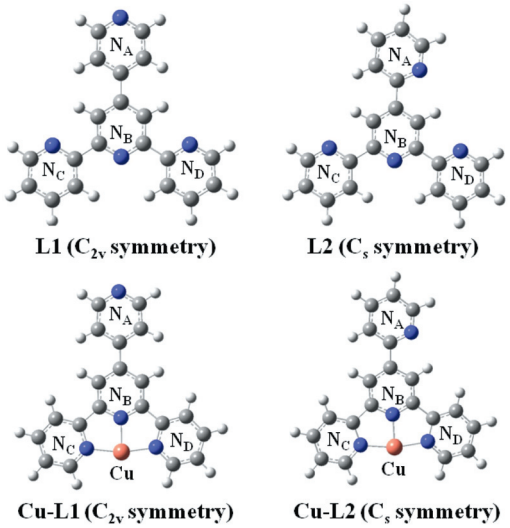

Fig. 5 The optimized structures of **L1**, **L2** and their complexes with Cu.

thus be represented as $[(Cu^{II}Br_2\mathbf{L2}Me)^+(Cu^{I}_{2.68}Br_{3.68})^-]_2$. As shown in Fig. 4, the Cu^I atoms are coordinated by the Br atoms and form a $Cu^I_6Br_8^-$ anionic cluster, which further links to two $Cu^{II}Br_2\mathbf{L2}Me^+$ species giving the eight-nuclear mixed-valence copper complex **4**. Unlike **1** and **2**, complex **4** is not further linked to Br^- to form a coordination polymer.

DFT calculations

The selective *N*-methylation of the pendant pyridyl group (N_A over N_B, N_C and N_D, Fig. 5) is considered as the result of the nucleophilic attack of N_A to the cationic methyl group generated from methanol. In this selective nucleophilic reaction, two possible effects should not be ruled out for consideration: (i) does the electronic effect play a role, along with the steric effect, in this selectivity; (ii) does the copper coordination affect this selectivity? To gain insight into these aspects, preliminary density functional theory (DFT) calculations were performed. The optimized structures of the ligands and complexes are shown in Fig. 5, and the NBO (Natural Bond Order) charges of the N and Cu atoms are summarized in Table 1.

For (i), we have found, in both **L1** and **L2**, the negative charge of N_A does not differ drastically from those of N_B, N_C and N_D; in fact, the NBO charges of N_B, N_C and N_D are even slightly more negative. Also the charges of N_A in **L1** and **L2** show no notable difference from each other, indicating the electronic effect may not be responsible for the selective *N*-methylation, which has to be majorly attributed to the steric effect. For (ii), the chelating effect enables the conformational adjustment of N_B, N_C and N_D when coordinating to Cu (Fig. 5). The reactivity of N_A in Cu-**L1** is reduced (negative charge from −0.447 to −0.377 *e*), and in Cu-**L2** maintains largely unchanged (negative charge from −0.452 to −0.458 *e*). This hints that the selective *N*-methylation may take place simultaneously to, or before, the coordination of Cu.

Because of the large steric hindrance in **L2**, the *N*-alkylation of **L2** should be an arduous task under traditional conditions.

Table 1 NBO charge (in *e*) analysis

	Cu	N_A	N_B	N_C	N_D
L1	—	−0.447	−0.465	−0.465	−0.465
L2	—	−0.452	−0.467	−0.466	−0.457
Cu-**L1**	1.080	−0.377	−0.499	−0.560	−0.560
Cu-**L2**	1.079	−0.458	−0.499	−0.560	−0.561

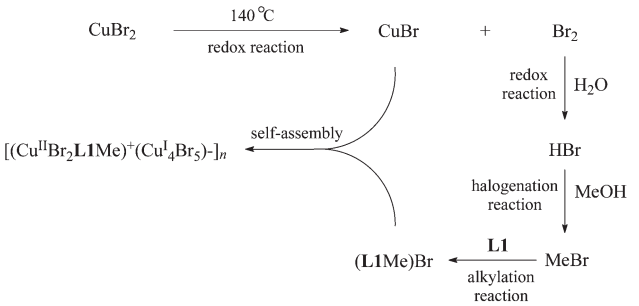

Scheme 1 Possible mechanism of alkylation of complex **1**.

This was verified by a recent report,[15] in which $[Ru(\mathbf{L2})_2][PF_6]_2$ is hardly *N*-alkylated (25 h at reflux in the presence of >1000-fold excess of MeI). In contrast, our present work shows that the *N*-alkylation of **L2** was successfully carried out even with alcohol under solvothermal conditions, where unusual organic reactions may happen.

Possible mechanism

Hydrothermal reactions of Cu^{II} with pyridylterpyridyl ligands *in situ* generate mixed-valence Cu^ICu^{II} compounds, where metal ions as redox agents may be crucial in promoting the ligand reactions. Self-assembly reactions of metal ions and the neutral pyridine-based 2,2′:6′,2″-terpyridine ligands adopted a unconventional solution method under extreme conditions, involving a simultaneous redox, *N*-methylation reactions. A rational assumption of the solvothermal reactions is similar to the situation previously reported by Yao *et al.*[12] Undoubtedly, the methyl group comes from methanol. Methanol acts directly as a sort of alkylation reagent. Another possible indirect sort of alkylation agent is MeBr when methanol was activated by Br_2 and H_2O. Br_2 is an important intermediate as oxidation products oxidated by Cu^{2+} ions. ESI-MS analyses confirmed that corresponding *N*-methylated compounds did exist in the reaction filtrates (Fig. S3, ESI†). As the UV-vis spectrum curves (Fig. S1, ESI†) display, ligand **L1** has three peaks at 240 nm, 276 nm, 312 nm, respectively while ligand **L2** has peaks at 241 nm, 279 nm, 312 nm. The spectra suggest that the reactions should produce new compounds because the curve of complex **1** has the new unique peak located in approximately 330 nm compared with the curves of the component and even the similar mixture with **L1** and $CuBr_2$ at room temperature. Regioselective alkylation of pendant pyridyl functionality *in situ* for complex molecule synthesis gave rise to $Cu^{II}Br_2\mathbf{L1}^+Me$, and anionic $Cu^I_nBr_{n+1}^-$ clusters which took the roles of charge balance (Scheme 1, complex **1** as an example).

Conclusion

In summary, we demonstrate a synthetic method to achieve homometallic mixed-valence copper(I/II) pyridine-based terpyridyl compounds formed by simultaneous *in situ* alkylation reactions of neutral ligands and redox cupric halides under solvothermal conditions in alcohol. All complexes were constructed of the $Cu^{II}Br_2$**L1**$^+$Me components and anionic $Cu^{I}{}_nBr_{n+1}{}^-$ clusters as counterions. These results show that the bifunctional ligand can accommodate both selective *N*-alkylation and coordination of added metal ions. In particular, the successful *N*-alkylation of the pendant 2-pyridyl of **L2** with a large steric hindrance suggests that such a method may be especially suitable and useful for enhancing some difficult organic reactions (*e.g.* the reagents or precursors with steric problems). Inspired by the successful *N*-alkylation of **L1** and **L2** with alcohol, the further *N*-alkylation on more amine molecules will be foreseen and exploited by the use of alcohol as the alkyl source under solvothermal conditions.

Experimental section

Materials and physical measurements

Chemicals and solvents used in this work were of analytical grade and used as purchased without further purification. NMR spectra were recorded on a Bruker AVANCE400 spectrometer and referenced to TMS. Infrared spectra were collected from a KBr disk on a Nicolet Avatar 360 FTIR spectrometer in the range of 4000–400 cm^{-1}. Elemental analyses of C, H, and N were determined with a Perkin-Elmer 2400C elemental analyzer. Thermogravimetric analysis (TGA) was carried out under argon atmosphere with the heating rate of 10 °C min^{-1} from room temperature to 800 °C on a Seiko Extar 6000 TG/DTA equipment. UV-vis measurements were performed using a Perkin-Elmer Lambda 35 spectrophotometer. ESI-MS analyses were carried out using an ABI4000 Q TRAP liquid chromatography-mass spectrometer.

Preparations

4′-(4-pyridyl)-2,2′:6′,2″-terpyridine (L1). A mixture of 4-pyridinecarboxaldehyde (3.21 g, 30 mmol), 2-acetylpyridine (7.26 g, 60 mmol) and solid NaOH (2.58 g, 62 mmol) was prepared using a pestle and mortar, the yellow medium aggregated until a yellow powder was formed (*ca*. 10 min) and then was further ground for 30 min. The powder was transferred to a suspension of ammonium acetate (20 g, excess) in glacial acetic acid (50 mL) and heated to reflux. After reaction for 3 h, a mixture of ethanol (30 mL) and water (40 mL) was added with stirring. Upon cooling, the crystalline product was precipitated from the solution, collected and recrystallized in ethanol to yield yellow crystals of **L1**. Yield: 4.28 g (46%, 13.8 mmol). m. p. 235 °C. Anal. Calcd for $C_{20}H_{14}N_4$: C, 77.40%; H, 4.55%; N, 18.05%. Found: C, 77.44%; H, 4.52%; N, 18.03%. ^{1}H NMR (400 MHz, $CDCl_3$) (Fig. S4, ESI†): δ = 8.79 (d, 2H, ^3J = 6.12 Hz), 8.09 (d, 2H, ^3J = 6.18 Hz), 8.01(s, 2H), 7.99(d, 2H, ^3J = 8.60 Hz), 7.87(d, 2H, ^3J = 8.42 Hz), 7.59 (m, 2H), 7.52 (m, 2H). IR (KBr, cm^{-1}) (Fig. S5, ESI†): 3052 w, 3007 w, 1581 s, 1548 m, 1467 m, 1393 m, 1070 w, 993 m, 780 m, in agreement with the literature data.[27,28]

4′-(2-Pyridyl)-2,2′:6′,2″-terpyridine (L2). It was prepared analogously to **L1** by replacing 4-acetylpyridine with 2-acetylpyridine in the same mole ratio. As a result, a yellow crystalline solid was obtained in 25% yield. m.p. 232 °C. Anal. Calc for $C_{20}H_{14}N_4$: C, 77.40%; H, 4.55%; N, 18.05%. Found: C, 77.45%; H, 4.51%; N, 18.01%. ^{1}H NMR (400 MHz, $CDCl_3$): δ = 9.11 (s, 2H), 8.81 (d, 1H, ^3J = 6.53 Hz), 8.75(d, 2H, ^3J = 7.43 Hz), 8.67(d, 2H, ^3J = 7.95 Hz), 8.08(d, 1H, ^3J = 7.96 Hz), 7.86 (m, 3H), 7.35 (m, 3H). IR (KBr, cm^{-1}): 3045 w, 1581 s, 1562 m, 1467 m, 1393 m, 1071 w, 982 m, 790 m.

$[(Cu^{II}Br_2L1Me)^+(Cu^{I}_4Br_5)^-]_n$ (1). A mixture of $CuBr_2$ (0.045 g, 0.2 mmol) and ligand **L1** (0.031 g, 0.1 mmol) in methanol (8 mL) was sealed in a 15 mL Teflon-lined reactor, heated to 140 °C for 72 h, and then cooled to room temperature at a rate of 6 °C h^{-1}. X-ray-quality black crystals of compound **1** were obtained in *ca*. 55% yield based on **L1**. Anal. Calcd for $C_{21}H_{17}Cu_5N_4Br_7$: C, 20.96%; H, 1.43%; N, 4.68%. Found: C, 21.01%; H, 1.41%; N, 4.66%. IR (KBr, cm^{-1}): 3035 w, 2922 w, 2850 w, 1635 m, 1614 m, 1558 s, 1472 w, 1415 m, 1242 s, 1017 m, 781 m, 508 m.

$[(Cu^{II}Br_2L1Me)^+(Cu^{I}_3Br_4)^-]_n$ (2). It was prepared analogously to compound **1** with double amounts of $CuBr_2$ (0.09 g, 0.4 mmol). Black crystals of compound **2** were obtained in *ca.* 25% yield (based on **L1**). Anal. Calcd for $C_{21}H_{17}Cu_4N_4Br_6$: C, 23.81%; H, 1.65%; N, 5.27%. Found: C, 23.79%; H, 1.62%; N, 5.31%. IR (KBr, cm^{-1}): 3055 w, 2927 w, 2855 w, 1718 w, 1699 m, 1636 m, 1559 m, 1541 s, 1410 w, 1228 m, 1016 s, 781 m, 705 m.

$[(Cu^{II}Br_2L1Me)^+(Cu^{I}Br_2)^-]$ (3). It was prepared analogously to compound **1** using $CuBr_2$ of 0.18 g (0.8 mmol). Black crystals of compound **3** were obtained in *ca.* 20% yield (based on **L1**). Anal. Calcd for $C_{21}H_{17}Cu_2N_4Br_4$: C, 32.68%; H, 2.25%; N, 7.21%. Found: C, 32.64%; H, 2.28%; N, 7.26%. IR (KBr, cm^{-1}): 3037 w, 2924 w, 2851 w, 1635 w, 1605 m, 1559 m, 1472 s, 1411 w, 1242 m, 1015 s, 783 m, 506 m.

$[(Cu^{II}Br_2L2Me)^+(Cu^{I}_{2.68}Br_{3.68})^-]_2$ (4). It was prepared analogously to compound **2** by replacing ligand **L1** with **L2**. Black crystals of compound **4** were obtained in *ca.* 45% yield based on **L2**. Anal. Calcd for $C_{42}H_{34}Br_{11.36}Cu_{7.36}N_8$: C, 24.90%; H, 1.69%; N, 5.53%. Found: C, 24.82%; H, 1.62%; N, 5.49%. IR (KBr, cm^{-1}): 3040 w, 2922 w, 2852 w, 1654 w, 1636 m, 1599 m, 1560 s, 1466 w, 1408 m,1245 m, 1016 s, 776 m, 721 m.

X-ray crystallography

Suitable crystals of **1–4** were mounted with glue at the end of a glass fiber, respectively. Diffraction data was collected at 293(2) K with a Bruker-AXS SMART CCD area detector diffractometer using ω rotation scans with a scan width of 0.3° and Mo-Kα radiation (λ = 0.71073 Å). Multi-scan absorptions were applied. Reflection intensities were integrated using SAINT software, and an absorption correction was applied. The structures were solved by the direct methods and refined by full-matrix least-squares

Table 2 Crystal data and structure refinement parameters for complexes **1–4**

	1	**2**	**3**	**4**
Formula	$C_{21}H_{17}Br_7Cu_5N_4$	$C_{21}H_{17}Br_6Cu_4N_4$	$C_{21}H_{17}Br_4Cu_2N_4$	$C_{42}H_{34}Br_{11.36}Cu_{7.36}N_8$
M_r	1202.46	1059.01	772.11	2026.18
Cryst syst	Monoclinic	Monoclinic	Triclinic	Monoclinic
Space group	$C2/c$	$P2(1)/c$	$P\bar{1}$	$C2/c$
a (Å)	10.3551(9)	9.3227(8)	9.724(2)	33.656(8)
b (Å)	27.263(2)	8.3368(8)	11.040(3)	9.029(2)
c (Å)	11.1239(10)	35.520(3)	12.238(3)	18.153(4)
α (°)	90	90	71.211(4)	90
β (°)	112.780(2)	91.218(2)	83.308(4)	90.725(4)
γ (°)	90	90	65.455(4)	90
V (Å^3)	2895.5(4)	2760.0(4)	1131.2(5)	5516(2)
Z	4	4	2	4
D_c (g cm^{-3})	2.758	2.549	2.267	2.439
μ (mm^{-1})	13.294	11.746	8.962	11.045
No. of reflns collected	8883	13 831	8156	15 330
No. of unique reflns	3264	4830	3952	4696
R_{int}	0.0443	0.0533	0.0359	0.0573
GOF	1.048	1.082	0.975	1.054
R_1 $[I > 2\sigma(I)]^a$	0.0484	0.0504	0.0395	0.0546
wR_2 $[I > 2\sigma(I)]^b$	0.1214	0.1283	0.0885	0.1401
R_1 [all data]^a	0.0757	0.0729	0.0564	0.0813
wR_2 [all data]^b	0.1466	0.1468	0.0975	0.1596

^{a} $R_1 = \sum(||F_o| - |F_c||) / \sum|F_o|$. ^{b} $wR_2 = [\sum w(F_o^2 - F_c^2)^2 / \sum w(F_o^2)^2]^{1/2}$.

refinements based on F^2. All non-hydrogen atoms were refined with anisotropic thermal parameters, and all hydrogen atoms were included in calculated positions and refined with isotropic thermal parameters riding on those of the parent atoms. Structure solutions and refinements were performed with the SHELXL-97 package.[29] The parameters and experimental details of crystals **1–4** are summarized in Table 2.

DFT calculation

Density functional theory calculations were performed using the Gaussian09 A.02 program package[30] at the B3LYP[31] level. For the geometric optimization and NBO[32] charge analysis, the 6-31G(d)[33] basis set was used for C, N and H elements, while the SDD[34] effective core potential (ECP) and basis set were used for Cu element.

Acknowledgements

This work was financially supported by the National Science Foundation for Distinguished Young Scholars of China (Grant No. 20825102) and the National Natural Science Foundation of China (Grant Nos. 20771072, 21171114 and 21101103).

References

1 X. M. Chen and M. L. Tong, *Acc. Chem. Res.*, 2007, **40**, 162.
2 (*a*) X. M. Zhang, *Coord. Chem. Rev.*, 2005, **249**, 1201; (*b*) M. I. H. Mohideen, B. Xiao, P. S. Wheatley, A. C. Mckinlay, Y. Li, A. M. Z. Slawin, D. W. Aldous, N. F. Cessford, T. Düren, X. B. Zhao, R. Gill, K. M. Thomas, J. M. Griffin, S. E. Ashbrook and R. E. Morris, *Nat. Chem.*, 2011, **3**, 304.
3 O. R. Evans and W. B. Lin, *Acc. Chem. Res.*, 2002, **35**, 511.
4 (*a*) X. M. Zhang, M. L. Tong and X. M. Chen, *Angew. Chem., Int. Ed.*, 2002, **41**, 1029; (*b*) A. Gallego, O. Castillo, C. J. Gómez-García, F. Zamora and S. Delgado, *Inorg. Chem.*, 2012, **51**, 718; (*c*) C. P. Li, X. H. Zhao, X. D. Chen, Q. Yu and M. Du, *Cryst. Growth Des.*, 2010, **10**, 5034.
5 N. Zheng, X. Bu and P. Feng, *J. Am. Chem. Soc.*, 2002, **124**, 9688.
6 J. P. Zhang, S. L. Zheng, X. C. Huang and X. M. Chen, *Angew. Chem., Int. Ed.*, 2004, **43**, 206.
7 J. P. Zhang, Y. Y. Lin, X. C. Huang and X. M. Chen, *J. Am. Chem. Soc.*, 2005, **127**, 5495.
8 R. Peng, M. Li and D. Li, *Coord. Chem. Rev.*, 2010, **254**, 1.
9 K. I. Fujita, Z. Li, N. Ozekib and R. Yamaguchib, *Tetrahedron Lett.*, 2003, **44**, 2687.
10 S. Bähn, S. Imm, K. Mevius, L. Neubert, A. Tillack, J. M. J. Williams and M. Beller, *Chem.–Eur. J.*, 2010, **16**, 3590.
11 (*a*) T. Wu, M. Li, D. Li and X. C. Huang, *Cryst. Growth Des.*, 2008, **8**, 568; (*b*) Y. Cheng, P. Xu, Y. B. Ding and Y. G. Yin, *CrystEngComm*, 2011, **13**, 2644; (*c*) Y. Du, S. Oishi and S. Saito, *Chem.–Eur. J.*, 2011, **17**, 12262; (*d*) F. Li, H. X. Shan, Q. K. Kang and L. Chen, *Chem. Commun.*, 2011, **47**, 5058.
12 J. K. Cheng, Y. G. Yao, J. Zhang, Z. J. Li, Z. W. Cai, X. Y. Zhang, Z. N. Chen, Y. B. Chen, Y. Kang, Y. Y. Qin and Y. H. Wen, *J. Am. Chem. Soc.*, 2004, **126**, 7796.
13 G. Xu, G. C. Guo, M. S. Wang, Z. J. Zhang, W. T. Chen and J. S. Huang, *Angew. Chem., Int. Ed.*, 2007, **46**, 3249.
14 Z. J. Zhang, S. C. Xiang, G. C. Guo, G. Xu, M. S. Wang, J. P. Zou, S. P. Guo and J. S. Huang, *Angew. Chem., Int. Ed.*, 2008, **47**, 4149.
15 J. E. Beves, E. I. Dunphy, E. C. Constable, C. E. Housecroft, C. J. Kepert, M. Neuburger, D. J. Price and S. Schaffner, *Dalton Trans.*, 2008, 386.
16 E. C. Constable, E. L. Dunphy, C. E. Housecroft, W. Kylberg, M. Neuburger, S. Schaffner, E. R. Schofield and C. B. Smith, *Chem.–Eur. J.*, 2006, **12**, 4600.
17 L. Hou, D. Li, W. J. Shi, Y. G. Yin and S. W. Ng, *Inorg. Chem.*, 2005, **44**, 7825.
18 H. Feng, X. P. Zhou, T. Wu, D. Li, Y. G. Yin and S. W. Ng, *Inorg. Chim. Acta*, 2006, **359**, 4027.
19 S. S. Zhang, S. Z. Zhan, M. Li, R. Peng and D. Li, *Inorg. Chem.*, 2007, **46**, 4365.
20 X. P. Zhou, W. X. Ni, S. Z. Zhan, J. Ni, D. Li and Y. G. Yin, *Inorg. Chem.*, 2007, **46**, 2345.
21 X. Z. Li, M. Li, Z. Li, J. Z. Hou, X. C. Huang and D. Li, *Angew. Chem., Int. Ed.*, 2008, **47**, 6371.
22 B. M. Wellsa, C. P. Landeea, M. M. Turnbulla, F. F. Awwadib and B. Twamley, *J. Mol. Catal. A: Chem.*, 2005, **228**, 117.
23 B. L. Chen, K. F. Mok and S. C. Ng, *J. Chem. Soc., Dalton Trans.*, 1998, 2861.

24 J. G. Lin, Y. Y. Xu, L. Qiu, S. Q. Zang, C. S. Lu, C. Y. Duan, Y. Z. Li, S. Gao and Q. J. Meng, *Chem. Commun.*, 2008, 2659.
25 R. P. Feazell, C. E. Carson and K. K. Klausmeyer, *Inorg. Chem.*, 2006, **45**, 2627.
26 K. L. Gurunatha, K. Uemura and T. K. Maji, *Inorg. Chem.*, 2008, **47**, 6578.
27 G. W. V. Cave and C. L. Raston, *J. Chem. Soc., Perkin Trans., 1*, 2001, 3258.
28 J. Wang and G. S. Hanan, *Synlett*, 2005, 1251.
29 G. M. Sheldrick, *SHELXL-97, Program for refinement of crystal structures*, University of Göttingen, Germany, 1997.
30 M. J. Frisch, G. W. Trucks, H. B. Schlegel, G. E. Scuseria, M. A. Robb, J. R. Cheeseman, G. Scalmani, V. Barone, B. Mennucci, G. A. Petersson, H. Nakatsuji, M. Caricato, X. Li, H. P. Hratchian, A. F. Izmaylov, J. Bloino, G. Zheng, J. L. Sonnenberg, M. Hada, M. Ehara, K. Toyota, R. Fukuda, J. Hasegawa, M. Ishida, T. Nakajima, Y. Honda, O. Kitao, H. Nakai, T. Vreven, J. A. Montgomery, Jr., J. E. Peralta, F. Ogliaro, M. Bearpark, J. J. Heyd, E. Brothers, K. N. Kudin, V. N. Staroverov, R. Kobayashi, J. Normand, K. Raghavachari, A. Rendell, J. C. Burant, S. S. Iyengar, J. Tomasi, M. Cossi, N. Rega, J. M. Millam, M. Klene, J. E. Knox, J. B. Cross, V. Bakken, C. Adamo, J. Jaramillo, R. Gomperts, R. E. Stratmann, O. Yazyev, A. J. Austin, R. Cammi, C. Pomelli, J. Ochterski, R. L. Martin, K. Morokuma, V. G. Zakrzewski, G. A. Voth, P. Salvador, J. J. Dannenberg, S. Dapprich, A. D. Daniels, O. Farkas, J. B. Foresman, J. V. Ortiz, J. Cioslowski and D. J. Fox, *GAUSSIAN 09 (Revision A.2)*, Gaussian, Inc., Wallingford, CT, 2009.
31 C. Lee, W. Yang and R. G. Parr, *Phys. Rev. B*, 1988, **37**, 785.
32 A. E. Reed, L. A. Curtiss and F. Weinhold, *Chem. Rev.*, 1988, **88**, 899.
33 (*a*) R. Ditchfield, W. J. Hehre and J. A. Pople, *J. Chem. Phys.*, 1971, **54**, 724; (*b*) W. J. Hehre, R. Ditchfield and J. A. Pople, *J. Chem. Phys.*, 1972, **56**, 2257; (*c*) P. C. Hariharan and J. A. Pople, *Theor. Chim. Acta*, 1973, **28**, 213; (*d*) P. C. Hariharan and J. A. Pople, *Mol. Phys.*, 1974, **27**, 209; (*e*) M. S. Gordon, *Chem. Phys. Lett.*, 1980, **76**, 163.
34 M. Dolg, U. Wedig, H. Stoll and H. Preuss, *J. Chem. Phys.*, 1987, **86**, 866.